iJRASET
International Journal For Research in Applied Science and Engineering Technology

INTERNATIONAL JOURNAL FOR RESEARCH
IN APPLIED SCIENCE & ENGINEERING TECHNOLOGY

Volume: 13 Issue: XII Month of publication: December 2025

DOI: https://doi.org/10.22214/ijraset.2025.76014

International Journal for Research in Applied Science & Engineering Technology (IJRASET)
ISSN: 2321-9653; IC Value: 45.98; SJ Impact Factor: 7.538
Volume 13 Issue XII Dec 2025- Available at www.ijraset.com

Study of Vortex Flow Phenomena in a Vortex Turbine Basin with Cone Angle Variations

I Putu Widiarta[1], Made Suarda[2], Made Sucipta[3], I Gusti Ketut Sukadana[4]
[1, 2, 3, 4]Mechanical Engineering Department, Udayana University

Abstract: Vortex turbines are widely developed due to their main advantages, namely their ability to operate at low flow heads and their simple construction design, making them suitable for application in mountainous rivers. The working principle of a vortex turbine is to utilize the energy of the vortex flow to rotate the turbine runner, thereby generating mechanical power for the vortex turbine. The runner blade profile functions to extract vortex flow energy into mechanical energy through momentum transfer, while the vortex turbine basin plays an important role in creating free vortex flow. Vortex turbine basins are generally cylindrical and conical in shape. Conical basins produce higher vortex turbine output power compared to cylindrical basins. cone angle of the conical basin significantly influences the vortex flow velocity gain. this study aims to analyse the phenomenon of free vortex flow pattern formation with variations in the cone angle basin with a constant d/D ratio and vortex head. The free vortex flow pattern study utilized Ansys software to conduct computational fluid flow (CFD). Cone angle variation of 10° produces a more even distribution of velocity and pressure. Dominant tangential velocity vector occurs in the cone angle variation of 10. The cone angle variation of 10 produces the highest average pressure value at the 66% basin position. Vortex flow analysis and applicative consideration aspects, it can be recommended to use a conical basin with cone angle of 10° to produce optimal turbine performance.
Keywords: vortex turbine, basin, cone angle, free vortex and flow pattern

I. INTRODUCTION

Energy is crucial to discuss in terms of availability, energy sources, and energy conversion processes. Fossil fuels are currently the primary energy source. The widespread use of fossil fuels can lead to increased air pollution [1]. This has triggered a shift to more environmentally friendly renewable energy sources and the availability of renewable and sustainable energy sources. Commonly utilized renewable energy sources include wind energy, solar energy, biomass, ocean wave energy, and hydropower. Water energy, readily accessible and continuously available, is an alternative solution for hydropower generation. Hydropower plants utilize the energy of water flow to drive turbines, producing mechanical energy that can be converted into electrical energy through generators [2]. Water turbines can be classified into several types, one of which is the vortex turbine. A vortex turbine utilizes vortex flow as the primary turbine driver.

Vortex turbines are widely developed due to their main advantages, namely their ability to operate at low flow heads and their simple construction design, making them suitable for application in mountainous rivers [3]. The working principle of a vortex turbine is to utilize the energy of the vortex flow to rotate the turbine runner, thereby generating mechanical power for the vortex turbine (output power). The turbine output power can be transmitted through the turbine shaft to be used to rotate the generator [4]. The greater the output power produced by the turbine, the greater the turbine efficiency [5]. The effectiveness of a vortex turbine's power production is greatly influenced by the runner blade profile parameters and the shape of the vortex turbine basin [6]. The runner blade profile functions to extract vortex flow energy into mechanical energy through momentum transfer, while the vortex turbine basin plays an important role in creating free vortex flow [7]. The dimensions and shape of the vortex turbine basin are parameters that influence the formation of free vortex flow patterns [8].

Vortex turbine basins are generally cylindrical and conical in shape. Conical basins produce higher vortex turbine output power compared to cylindrical basins [9]. The basin parameter that influences the increase in vortex turbine output power is the ratio of the basin outlet diameter to the basin inlet diameter (d/D). A lower d/D ratio in a conical basin reduces the flow area, thereby increasing the vortex flow velocity and vortex strength [10]. Optimal vortex flow is formed with a basin outlet diameter 14% - 18% smaller than the basin inlet diameter [11]. According to Dhakal et al., (2020), a turbine basin with a d/D ratio of 20% - 25% is the effective ratio of a vortex turbine basin to produce optimal turbine output power [12]. Meanwhile, the height and diameter of the cylindrical basin outlet significantly affect the tangential, radial, and axial velocity gain, and the formation of air core [13]. The cone angle of the conical basin significantly influences the vortex flow velocity gain [14].

Jiang et al., (2022) have conducted a CFD (Computational Fluid Dynamics) simulation study by varying the cone angle of the turbine basin. A cone angle of 14° produces a higher velocity increment compared to cone angles of 13° and 15° [15]. However, this study has not tested the pressure distribution and flow patterns formed within the vortex turbine basin. The flow pattern can determine the direction of the flow velocity, namely tangential or axial. In a vortex turbine, tangential flow is the dominant parameter in the energy conversion process through the turbine runner.

Based on previous research, this study aims to analyse the phenomenon of free vortex flow pattern formation with variations in the cone angle basin with a constant d/D ratio and vortex head. Testing was carried out without a runner so that the pure characteristics of the free vortex flow in the turbine basin could be known and analysed. The free vortex flow pattern study utilized Ansys software to conduct computational fluid flow (CFD) where the CFD simulation was completed using the fluent solver. This study is expected to provide recommendations for optimal basin design seen from the aspects of flow formation and technical application considerations.

II. METHODOLOGY

A. Research Schematic

A vortex turbine is a turbine that utilizes low-head fluid flow as the primary driving energy source for the turbine. The vortex flow created in the vortex turbine basin is used to rotate the runner so that the turbine runner produces output power. The output power of the vortex turbine is in the form of shaft work that can be converted into electrical energy through a generator. In this study, the basin cone angle was varied with values of 0° (cylindrical), 5°, 10° and 20° to obtain the analysis of free vortex flow formation in the basin. The variations in the basin cone angle are shown in Figure 1 and the channel design is shown in Figure 2. Where the angle is in degrees (°) and the diameter and length are in mm. Each cone angle variation was simulated at the same head and d/D ratio conditions and tested at the theoretical maximum mass flow rate conditions.

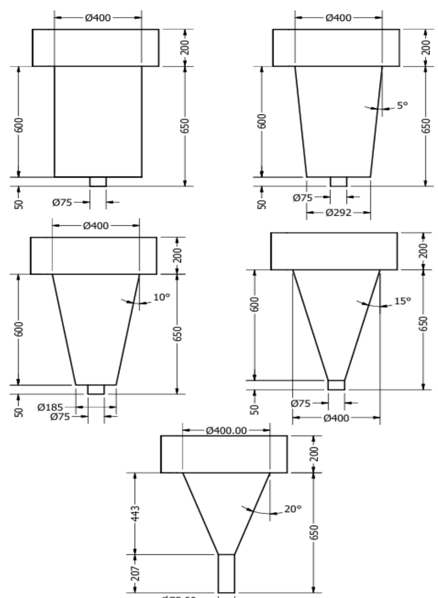

Fig. 1 Dimension and cone angle of vortex turbine basin

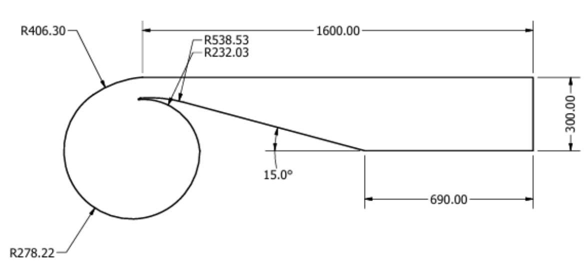

Fig. 2 Dimension of canal vortex turbine

International Journal for Research in Applied Science & Engineering Technology (IJRASET)
ISSN: 2321-9653; IC Value: 45.98; SJ Impact Factor: 7.538
Volume 13 Issue XII Dec 2025- Available at www.ijraset.com

B. CFD Modelling

The CFD (Computational Fluid Dynamics) simulation process is divided into several stages, including pre-processing, solving, and post-processing. Pre-processing is the process of determining the fluid domain and the meshing process. The meshing process uses a poly-hexcore mesh type, where this mesh type is a combination of poly and hexcore mesh types. The meshing process is carried out using the minimum and maximum size of the cells, and each test variation is meshed with the same parameters. Figures 3 and 4 are the fluid domain and poly-hexcore mesh type, respectively. Table 1 is the statistical data from the meshing results.

Table. 1 Grid data statistic

Cylindrical (0°)	Cells	822943
	Face	3335937
	Nodes	1852934
	Minimum Orthogonal Quality	0.2
	Average Orthogonal Quality	0.97
Conical (5°)	Cells	783948
	Face	3040392
	Nodes	1597030
	Minimum Orthogonal Quality	0.15
	Average Orthogonal Quality	0.97
Conical (10°)	Cells	725798
	Face	2838162
	Nodes	1507925
	Minimum Orthogonal Quality	0.14
	Average Orthogonal Quality	0.97
Conical (15°)	Cells	680910
	Face	2675716
	Nodes	1428586
	Minimum Orthogonal Quality	0.2
	Average Orthogonal Quality	0.97
Conical (20°)	Cells	652140
	Face	2570643
	Nodes	1378114
	Minimum Orthogonal Quality	0.19
	Average Orthogonal Quality	0.97

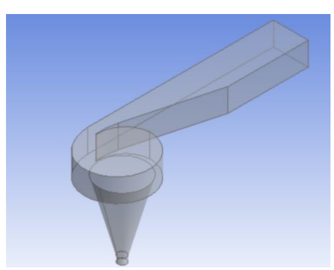

Fig. 3 Fluid domain

International Journal for Research in Applied Science & Engineering Technology (IJRASET)
ISSN: 2321-9653; IC Value: 45.98; SJ Impact Factor: 7.538
Volume 13 Issue XII Dec 2025- Available at www.ijraset.com

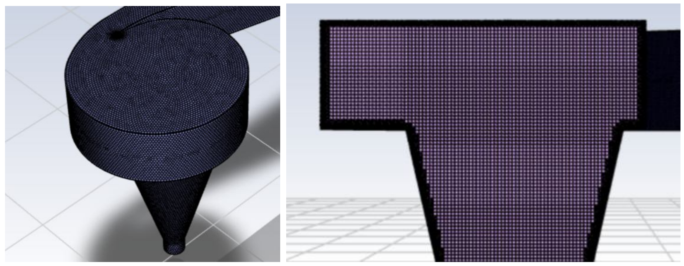

Fig. 4 Poly hexcore mesh result.

The solving process is to determine the CFD simulation boundary conditions and determine the solver scheme used to complete the fluid motion computation. The solver scheme used is SIMPLE (Semi Implicit Pressure Linked Equation) with spatial discretization, namely second order upwind on pressure, momentum, turbulent kinetic energy and specific dissipation rate. The simulation boundary conditions, namely inlet, outlet and wall, are each shown in Figure 5. The inlet condition is set up as a mass flow rate; the outlet condition is set up as a pressure outlet with a pressure value of 1 atmosphere and the wall is set up as a no slip condition. The fluid viscosity model used is the k-omega SST (Shear Stress Transport) model.

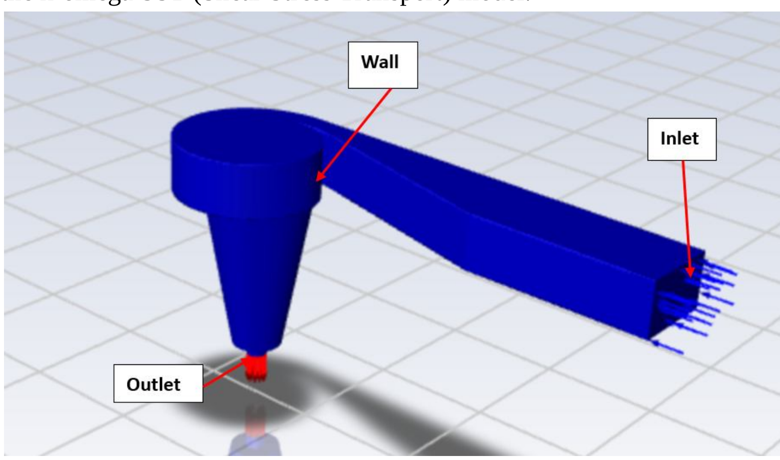

Fig. 5 Boundary condition

C. Calculation of the theoretical maximum capacity of a vortex turbine

The theoretical maximum capacity of a vortex turbine can be calculated using the Bernoulli equation. The Bernoulli equation relates the fluid energy conditions from the inlet to the outlet of the system, thus calculating the fluid energy at the outlet side [16].

$$\frac{P_1}{\rho g} + \frac{V_1^2}{2g} + Z_1 = \frac{P_2}{\rho g} + \frac{V_2^2}{2g} + Z_2 \quad (1)$$

$$Vmax = v_2 = \sqrt{2gh} \quad (2)$$

Theoretical maximum capacity (Qmax) of the vortex turbine can be calculated using the continuity equation.

$$Qmax = V_{max}.A_{outlet} \quad (3)$$

Where g is gravitation acceleration (m/s^2), h is the elevation (m), $Vmax$ is the maximum velocity on outlet basin (m/s), A_{outlet} define as area of outlet basin (m^2) and $Qmax$ is the maximum theoretical capacity (m^3/s). In this study, the input to the inlet boundary condition is the mass flow rate. The mass flow rate can be calculated by multiplying the theoretical maximum capacity (Qmax) by the fluid density (ρ). Therefore, the input to the inlet condition is the theoretical maximum mass flow rate. Each cone angle variation was tested at 100% of the theoretical maximum capacity of the vortex turbine.

International Journal for Research in Applied Science & Engineering Technology (IJRASET)
ISSN: 2321-9653; IC Value: 45.98; SJ Impact Factor: 7.538
Volume 13 Issue XII Dec 2025- Available at www.ijraset.com

III.RESULT AND DISCUSSION

The CFD simulation residuals generated for each cone angle variation are 10-5 for the momentum equation (x, y, and z directions). The resulting CFD simulation residuals are able to achieve the predetermined convergence target with 1000 iterations.

A. Velocity and Pressure Contour

Pressure and velocity contours were taken on 5 horizontal planes in the basin with each distance of 10 cm. Figures 6 and 7 show the distribution of pressure contours and vortex flow velocity in the vortex turbine basin. Sub-numbers a, b, c, d and e respectively indicate the variations of the basin cone angle, namely 0°, 5°, 10°, 15° and 20°. Figure 6 shows that the most even pressure distribution occurs in the 0° cone angle variation (cylindrical) but the pressure value is lower than the conical basin at each cone angle variation. In the conical basin model, the 10° cone angle variation produces a more even pressure distribution compared to the 5°, 15° and 20° variations. An even pressure distribution indicates that the flow energy from the fluid is evenly distributed in the vortex turbine basin. This ensures that the blade runner area receives flow energy evenly. Furthermore, the amount of flow energy in the form of fluid pressure can influence the amount of energy conversion that can be generated through the turbine runner.

Figure 7 shows the distribution of velocity contours and sub numbers a, b, c, d, and e are the cone angle variations of 0°, 5°, 10°, 15°, and 20°, respectively. In general, the conical basin model produces higher velocity values compared to the cylindrical basin model. The highest velocity occurs at a cone angle variation of 20°, but the velocity is not evenly distributed in the turbine basin. Cone angle variations of 10° and 15° produce a more even velocity distribution compared to the 20° cone angle variation. Increasing the basin cone angle can increase the flow velocity value because there is a narrowing of the flow area in the basin, so that the fluid velocity increases. The low velocity contour at the centre basin indicates the formation of air core in the vortex turbine basin. Increasing the cone angle of the conical basin causes air core to occur closer to the inlet area of the basin, but at a cone angle variation of 20°, air core does not form in the turbine basin. According to Mulligent (2018), one of the parameters of a strong vortex flow is the formation of a stable air core [11].

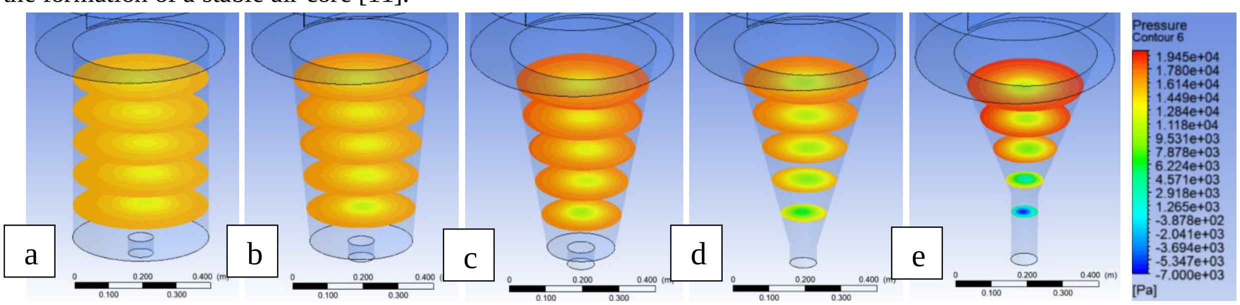

Fig. 6 Pressure contour

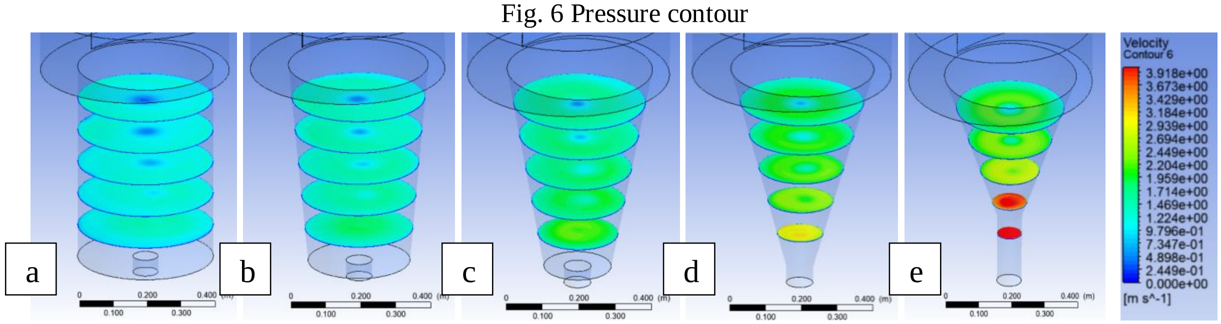

Fig .7 Velocity contour

B. Velocity vector

Velocity vectors were observed in each cone angle basin variation. Figure 8 shows the velocity vectors in each cone angle basin variation of the vortex turbine. Sub-numbers a, b, c, d, and e indicate the cone angle variations of 0°, 5°, 10°, 15°, and 20°, respectively. In general, the highest velocity vector value occurs in the basin with a cone angle of 20° and the lowest value occurs in the 0° (cylindrical) variation. Increasing the cone angle can increase the value of the fluid flow velocity, but the velocity vector also has a direction of flow velocity. The velocity vectors in the cone angle variations of 20° and 15° show a tendency for several vectors to point towards the axial collar of the flow, so that in that area the axial flow is dominant. The cone angle variations 10° produce a uniform velocity vector pattern pointing towards the tangential flow, so that the flow is dominated by tangential flow.

International Journal for Research in Applied Science & Engineering Technology (IJRASET)
ISSN: 2321-9653; IC Value: 45.98; SJ Impact Factor: 7.538
Volume 13 Issue XII Dec 2025- Available at www.ijraset.com

A vortex turbine is a turbine that utilizes the tangential velocity of the vortex flow to move the runner so that a more even tangential velocity pattern is expected to occur in the vortex turbine basin [17]. The increasing value of the tangential velocity of the vortex flow increases the turbine rotation. At a cone angle variation of 0°, 5° -15°, several vectors have low values, this phenomenon indicates the presence of flow yield in areas with low velocity vector values due to the presence of blockage mass near the outlet basin area.

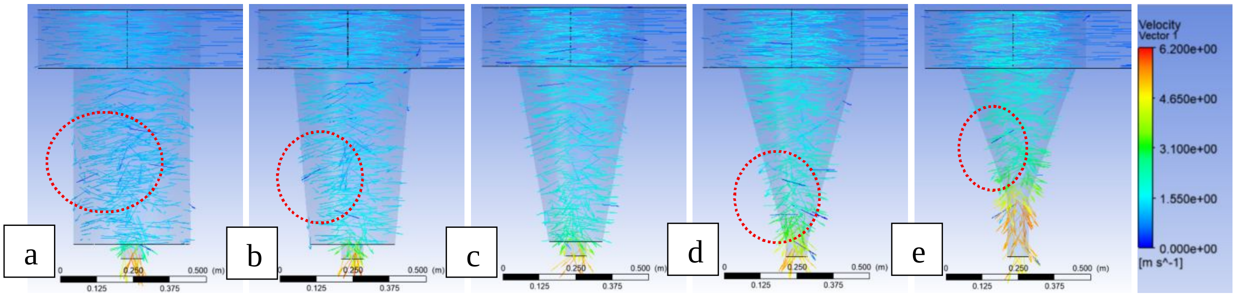

Fig. 8 Velocity vector

C. Streamline

The flow streamline was created with 100 tracking points at each cone angle basin variation to determine the fluid flow path. Figure 9 shows the flow streamline and sub-numbers a, b, c, d and e are the cone angle variations of 0°, 5°, 10°, 15° and 20°, respectively. Increasing the cone angle of the turbine basin causes an increase in fluid velocity in the basin where the highest velocity occurs at the 20° cone angle variation and the lowest velocity occurs at the 0° cone angle variation (cylindrical). Visualization of the flow through the streamline shows that the 0° cone angle variation produces the largest air core diameter. Increasing the cone angle of the basin results in a reduction in the air core space. The 15° and 20° cone angle variations experience an increase in flow velocity around the air core and the whirlpool becomes smaller. This phenomenon indicates that the flow begins to overflow due to the significantly reduced basin volume. Excessively high air core space prevents the turbine runner from being fully exposed to the water flow [18]. This affects the conversion of vortex flow energy into mechanical energy in the runner, which is suboptimal because the projected flow area on the runner blades is reduced.

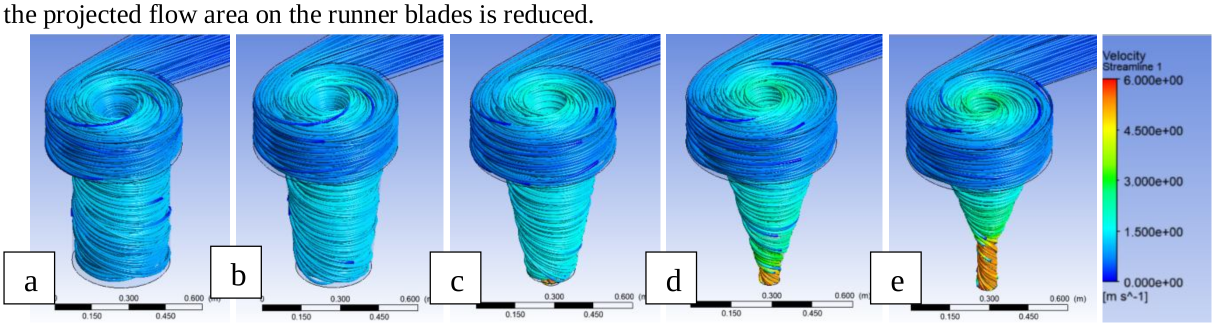

Fig. 9 Streamline.

D. Velocity distribution

The maximum velocity distribution in each horizontal plane can be made in the form of a graph as shown in Figure 10. Increasing the cone angle of the vortex turbine basin can cause the flow velocity distribution in the vortex turbine basin to increase. This is also found in the research conducted by Dhakkal, (2014) [19]. The cone angle variation of 20° produces the highest velocity distribution, but there is a significant difference in velocity values starting from the 50% - 80% position. The phenomenon of a significant increase in flow velocity indicates that the flow in the turbine basin with a cone angle of 20° is dominant in the axial direction due to the effect of a significant reduction in the flow area. On the other hand, the vortex turbine is a turbine that predominantly utilizes the tangential velocity of the vortex flow to drive the runner. The cone angle variations of 10°, 5° and 0° produce a more even velocity distribution compared to the cone angles of 20° and 15°. A more even velocity distribution indicates that the flow has a tendency towards the tangential vortex flow. The velocity distribution phenomenon can be observed from the velocity contour distribution as shown in Figure 7 and the velocity vector in Figure 8.

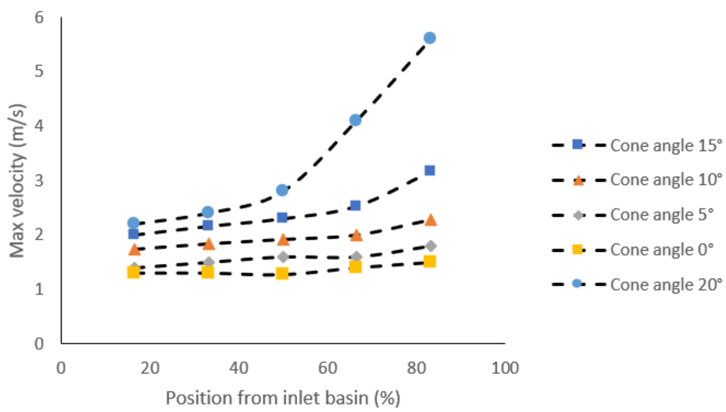

Fig. 10 Velocity distribution

Figure 11 shows the average velocity and increment in percentage. The variation of the cone angle affects the average velocity in the turbine basin where the higher the cone angle of the turbine basin causes an increase in the average velocity in the turbine basin. While the velocity increment is not linear. Variations of 0 to 10 show an increase in the flow velocity increment, but there is a decrease in the increment at the 15° cone angle variation. This is caused by the occurrence of flow braking at several points as shown in the velocity vector in Figure 8. The flow velocity increment increases again at the 20° cone angle variation due to an increase in the average flow velocity.

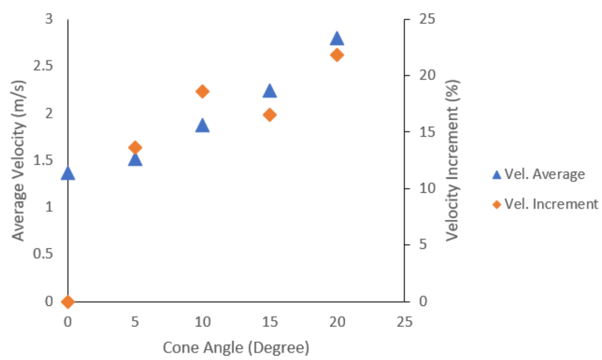

Fig. 11 Average velocity increament

E. Application consideration

Technical considerations for the application include the diameter of the vortex turbine runner that can be applied to each cone angle basin variation at a specific position. According to Dhakal, (2015) the optimal runner placement position in the conical basin is between 60% and 70% [3]. Therefore, a sketch of the potential runner blade area was performed for each cone angle variation at the 66% position with the same clearance in each variation. The sketch was performed using CAD software, Inventor. The sketch results for the potential runner design are shown in Table 2.

Table. 2 Potential diameter runner of vortex turbine in each basin model

Parameter	Various of Cone Angle				
	0	5	10	15	20
Diameter runner (m)	0.339568	0.285884	0.232424	0.17714	0.119186

Runner diameter is an important parameter in the magnitude of the energy conversion process in a vortex turbine. Under the same operational conditions, a larger runner diameter can produce higher torque than a smaller runner diameter. However, a runner diameter that is too high can cause the runner rotation to decrease. Turbine power is the product of the runner torque and the runner rotation (rad/s).

On the other hand, another parameter to consider is the vortex flow pressure value around the vortex turbine runner immersion position. The magnitude of the pressure value around the runner is the amount of potential energy that can be converted into mechanical energy by the turbine runner. Figure 12 shown average pressure at 66% posotion runner immersion. The increase in pressure value occurs from the cone angle variation of 0 to 10, however there is a decreasing trend in pressure value from the cone angle variation of 15 and 20. The increase in pressure value occurs from the cone angle variation of 0 to 10, but there is a decreasing trend in pressure value from the cone angle variations of 15 and 20. Thus, at the runner immersion position of 66%, the cone angle variation of 10 has the highest energy potential compared to the cone angle variations of 0°, 5°, 15°, and 20°. Based on free vortex flow analysis and application aspect considerations, the cone angle variation of 10 is better than variations of 0°, 5°, 15° and 20°.

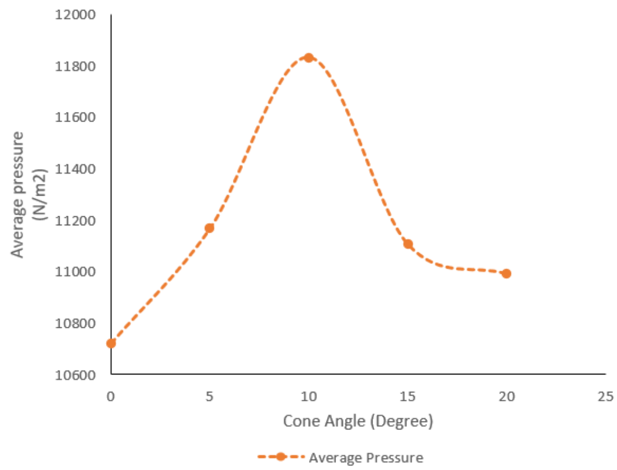

Fig. 12 Average pressure

IV. CONCLUSIONS

The cone angle variation of 10° produces a more even distribution of velocity and pressure compared to variations of 0°, 5°, 15° and 20°. The dominant tangential velocity vector occurs in the cone angle variation of 10. The cone angle variation of 10 produces the highest average pressure value at the 66% basin position compared to variations of 0°, 5°, 15° and 20°. From the vortex flow analysis and applicative consideration aspects, it can be recommended to use a conical basin with cone angle of 10° to produce optimal turbine performance.

V. ACKNOWLEDGMENT

The author would like to thank the Head of the Mechanical Achievement Laboratory, Faculty of Engineering, Udayana University for the research facilities.

REFERENCES

[1] Perera, F., & Nadeau, K. (2022). Climate Change, Fossil-Fuel Pollution, and Children's Health. New England Journal of Medicine, 386(24), 2303–2314. https://doi.org/10.1056/nejmra2117706

[2] Ng, S. K., Nakayama, A., & Ng, W. X. (2024). Application of Smoothed Particle Hydrodynamics Method for the Analysis of the Flow Past Vertical Vortex Turbine of a Micro Hydropower. KSCE Journal of Civil Engineering, 28(3), 1132–1139. https://doi.org/10.1007/s12205-024-1732-x

[3] Dhakal, S., Timilsina, A. B., Dhakal, R., Fuyal, D., Bajracharya, T. R., Pandit, H. P., Amatya, N., & Nakarmi, A. M. (2015). Comparison of cylindrical and conical basins with optimum position of runner: Gravitational water vortex power plant. In Renewable and Sustainable Energy Reviews (Vol. 48, pp. 662–669). Elsevier Ltd. https://doi.org/10.1016/j.rser.2015.04.030

[4] Rahman, M. M., Tan, J. H., Fadzlita, M. T., & Wan Khairul Muzammil, A. R. (2017). A Review on the Development of Gravitational Water Vortex Power Plant as Alternative Renewable Energy Resources. IOP Conference Series: Materials Science and Engineering, 217(1). https://doi.org/10.1088/1757-899X/217/1/012007

[5] Warjito, Ramadhan, A. A., Budiarso, Irwansyah, R., & Kurnianto, M. A. F. (2023). Performance Comparison of Straight, Curved, and Tilted Blades of Pico Scaled Vortex Turbine. CFD Letters, 15(2), 114–125. https://doi.org/10.37934/cfdl.15.2.114125

[6] Handoko, R., Septiyanto, M. D., Tjahjana, D. D. D. P., Himawanto, D. A., Yaningsih, I., & Hadi, S. (2023). Performance Testing and Analysis of Gravitational Water Vortex Turbine: A Modified Experimental Study on Blade Arc and Inclination Angle. Journal of Advanced Research in Fluid Mechanics and Thermal Sciences, 109(1), 147–161. https://doi.org/10.37934/arfmts.109.1.147161

[7] Kora, A. T., Ancha, V. R., & Tibba, G. S. (2022). Numerical analysis of the effect of runner-to-basin diameter ratio on the performance of gravitational water vortex turbine in a scroll basin. International Journal of Energy and Environmental Engineering, 13(4), 1317–1333. https://doi.org/10.1007/s40095-022-00495-4

[8] Ruiz Sánchez, A., Posada-Montoya, J. A., Tecnologico, I., Bravo, P., Andrés, J., Rio, S. Del, Guevara Muñoz, A. J., Alejandro, J., & Montoya, P. (2019). Numerical and Experimental Evaluation of Concave and Convex Designs for Gravitational Water Vortex Turbine. Journal of Advanced Research in Fluid Mechanics and Thermal Sciences Journal Homepage, 64, 160–172. www.akademiabaru.com/arfmts.html
[9] Aziz, M. Q. A., Idris, J., & Abdullah, M. F. (2022). Simulation Of the Conical Gravitational Water Vortex Turbine (GWVT) Design in Producing Optimum Force for Energy Production. Journal of Advanced Research in Fluid Mechanics and Thermal Sciences, 89(2), 77–91. https://doi.org/10.37934/arfmts.89.2.99113
[10] Fikri Musthapa, M., Mukhtar, A., Fariz, M., Nasir, M., & Tharima, A. F. (2020). Numerical Simulation of Micro Gravitational Hydro-turbine for Alternative Renewable Energy Resources in Rural Area (Vol. 2020).
[11] Mulligan, S., De Cesare, G., Casserly, J., & Sherlock, R. (2018). Understanding turbulent free-surface vortex flows using a Taylor-Couette flow analogy. Scientific Reports, 8(1). https://doi.org/10.1038/s41598-017-16950-w
[12] Dhakal, R., Shrestha, S., Neupane, H., Adhikari, S., & Bajracharya, T. (2020). Inlet and Outlet Geometrical Condition for Optimal Installation of Gravitational Water Vortex Power Plant with Conical Basin Structure. In Lecture Notes in Intelligent Transportation and Infrastructure: Vol. Part F1362 (pp. 163–174). Springer Nature. https://doi.org/10.1007/978-981-32-9971-9_17
[13] Chatta, J. A., Cheema, T. A., & Khan, N. H. (2017). The Eighth International Renewable Energy Congress (IREC) : 2017 8th International Renewable Energy Congress (IREC) : March 21-23, 2017 Amman - Jordan. IEEE.
[14] Zafar, U., Javid, W., Jamil, F., Iqbal, S., Ahmed, S., Aziz, A., & Mehmood, T. (2024). Comparative Study of Conical and Cylindrical Basins for Gravitational Water Vortex Turbines. 30. https://doi.org/10.3390/materproc2024017030
[15] Jiang, Y., Raji, A. P., Raja, V., Wang, F., Al-Bonsrulah, H. A. Z., Murugesan, R., & Ranganathan, S. (2022). Multi–Disciplinary Optimizations of Small-Scale Gravitational Vortex Hydropower (SGVHP) System through Computational Hydrodynamic and Hydro–Structural Analyses. Sustainability (Switzerland), 14(2). https://doi.org/10.3390/su14020727
[16] Sucipta, M., Sugita, I. K. G., & Anggarana, B. G. D. C. (2024). CFD simulation of vortex turbine performance with various water flow rates and number of runner blades. AIP Conference Proceedings, 2891(1). https://doi.org/10.1063/5.0201657
[17] Saleem, A. S., Cheema, T. A., Ullah, R., Ahmad, S. M., Chattha, J. A., Akbar, B., & Park, C. W. (2020). Parametric study of single-stage gravitational water vortex turbine with cylindrical basin. Energy, 200. https://doi.org/10.1016/j.energy.2020.117464
[18] Sinaga, D. A., Septiyanto, M. D., Arifin, Z., Rusdiyanto, G., Prasetyo, S. D., & Hadi, S. (2023). The Effect of Blade Distances on the Performance of Double-Stage Gravitational Water Vortex Turbine. Journal of Advanced Research in Fluid Mechanics and Thermal Sciences, 109(1), 196–209. https://doi.org/10.37934/arfmts.109.1.196209
[19] Dhakal, S., Timilsina, A. B., Dhakal, R., Timilsina, A. B., Dhakal, R., Fuyal, D., Ratna Bajracharya, T., & Pandit, H. P. (2014). Effect of Dominant Parameters for Conical Basin: Gravitational Water Vortex Power Plant. Proceeding of IOE Graduate Conference. https://doi.org/10.13140/RG.2.1.1455.7843

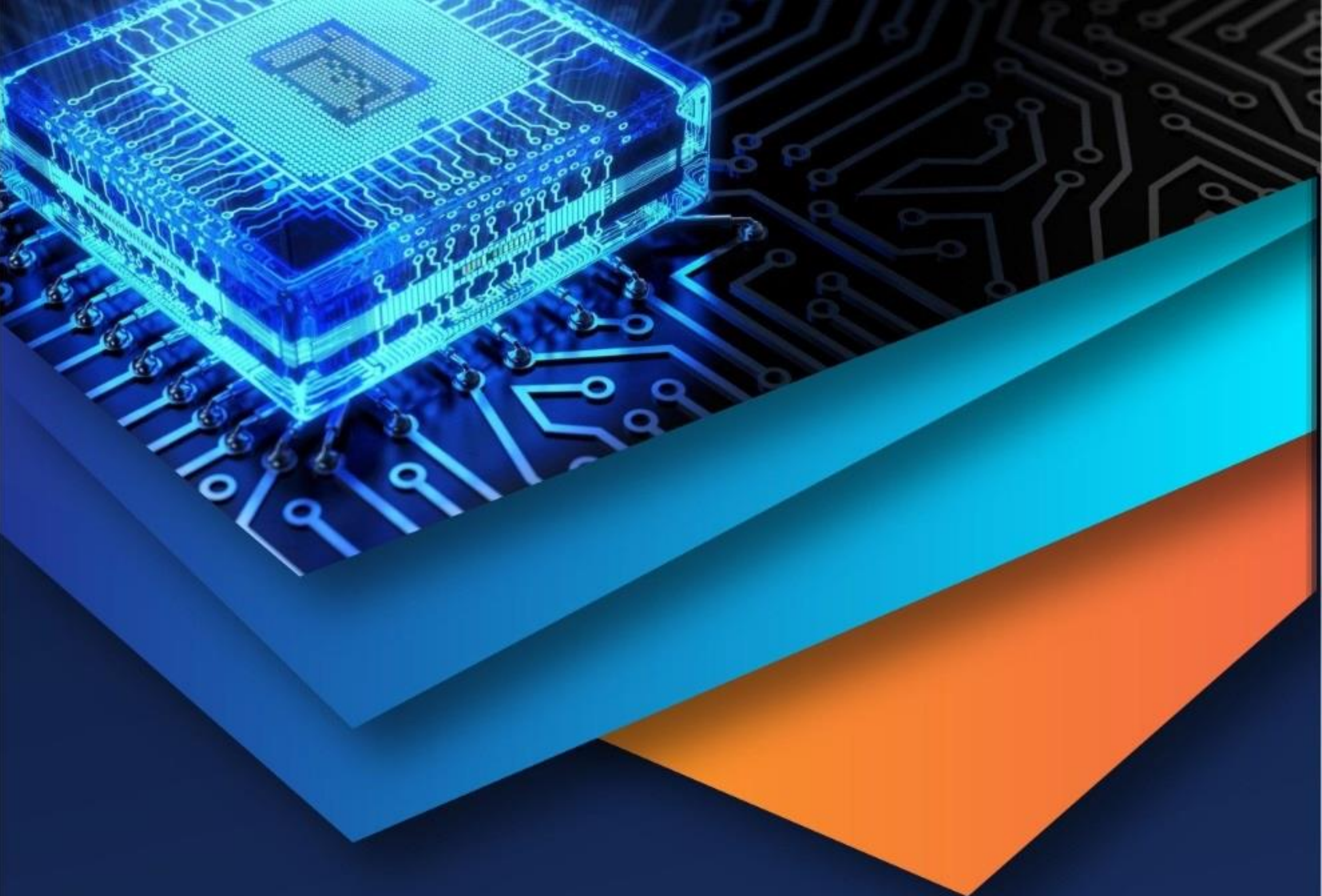

10.22214/IJRASET

INDEX COPERNICUS
45.98

IMPACT FACTOR:
7.129

TOGETHER WE REACH THE GOAL
IMPACT FACTOR:
7.429

INTERNATIONAL JOURNAL FOR RESEARCH

IN APPLIED SCIENCE & ENGINEERING TECHNOLOGY